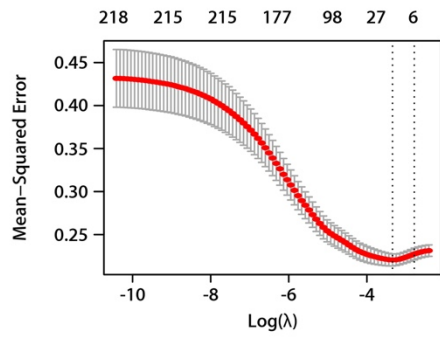


A



B

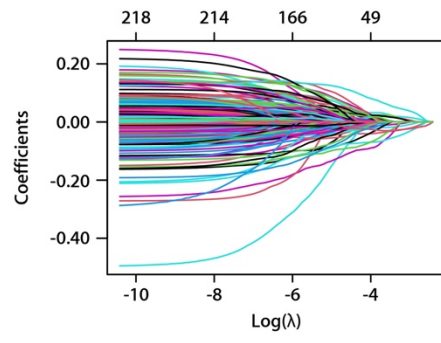


Fig. S1. LASSO regression analysis of the ROS-related genes.

(A) LASSO regression of the 235 ROS-related genes. (B) Cross-validation for tuning the parameter selection in the LASSO regression.

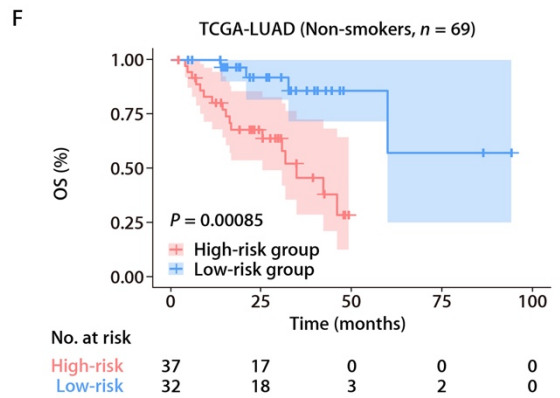
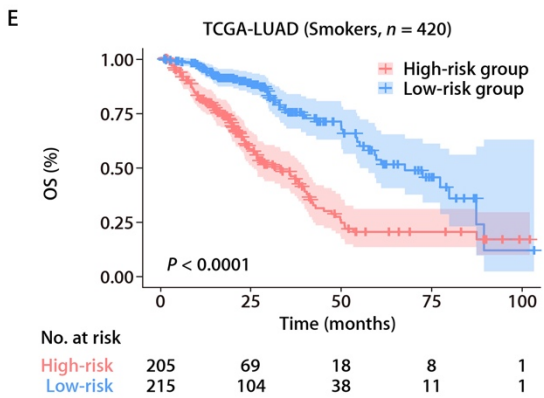
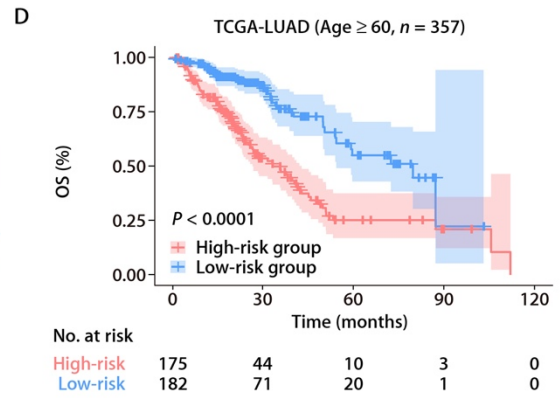
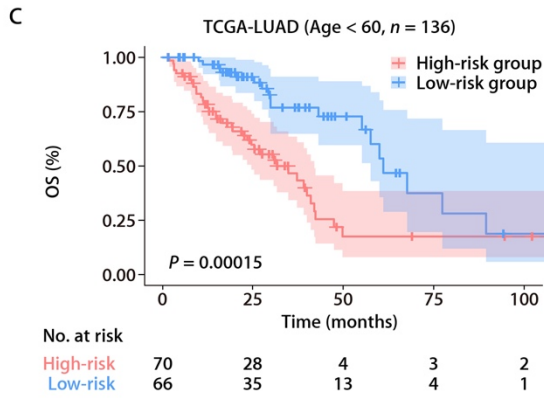
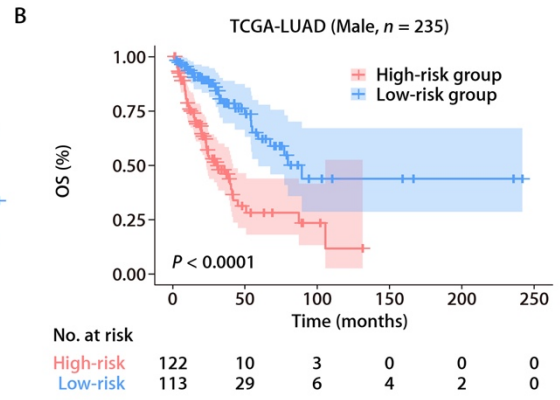
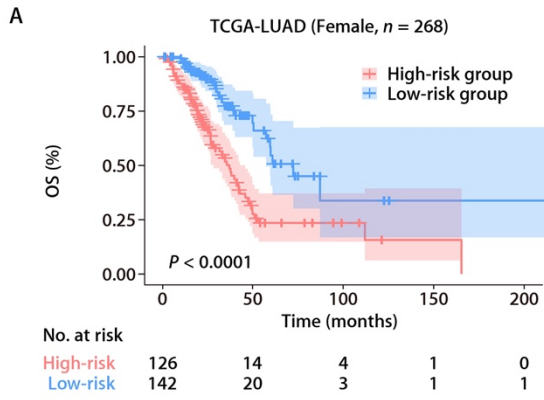


Fig. S2. Validation of the ROS-related signature in clinical subgroups.

K-M curves of OS in female (A), male (B), younger (C), older (D), smokers (E), and non-smokers (F) patients based on risk scores in TCGA-LUAD cohort.

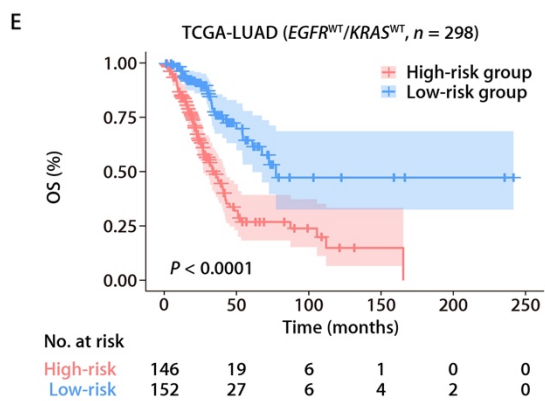
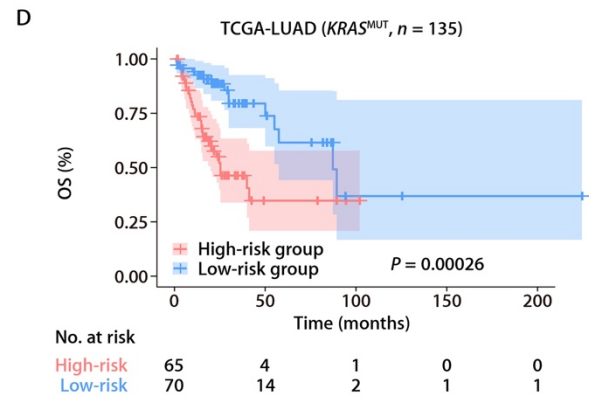
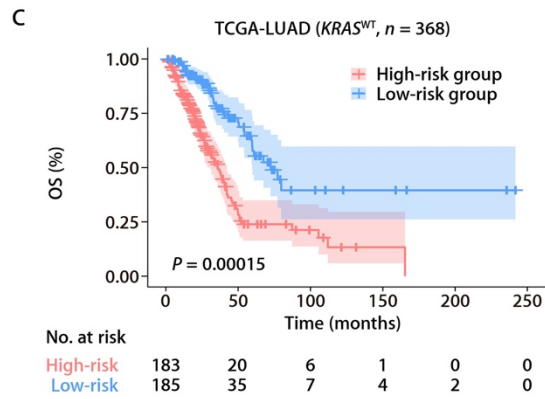
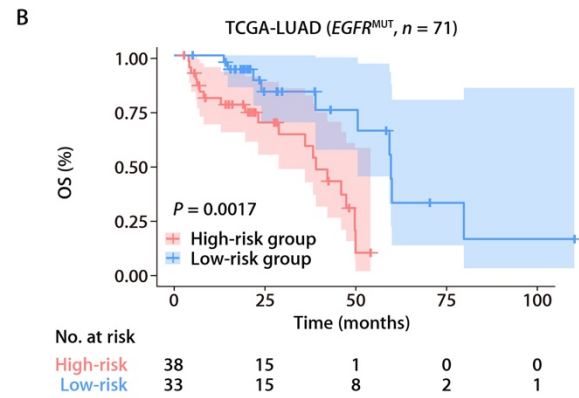
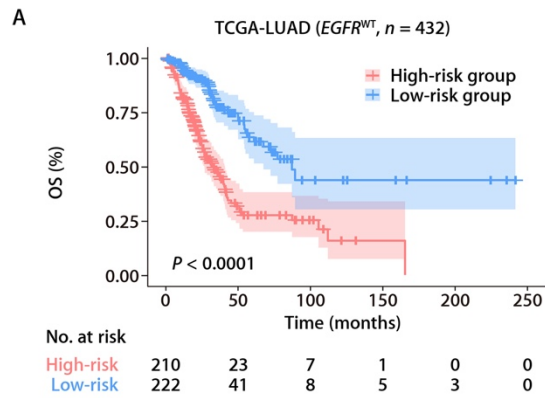


Fig. S3. Validation of the ROS-related signature in different mutation statuses.

K-M curves were plotted to estimate the OS for patients carrying $EGFR^{WT}$ (A), $EGFR^{MUT}$ (B), $KRAS^{WT}$ (C), $KRAS^{MUT}$ (D), and $EGFR^{WT}/KRAS^{WT}$ (E) based on the risk scores in TCGA-LUAD cohort.

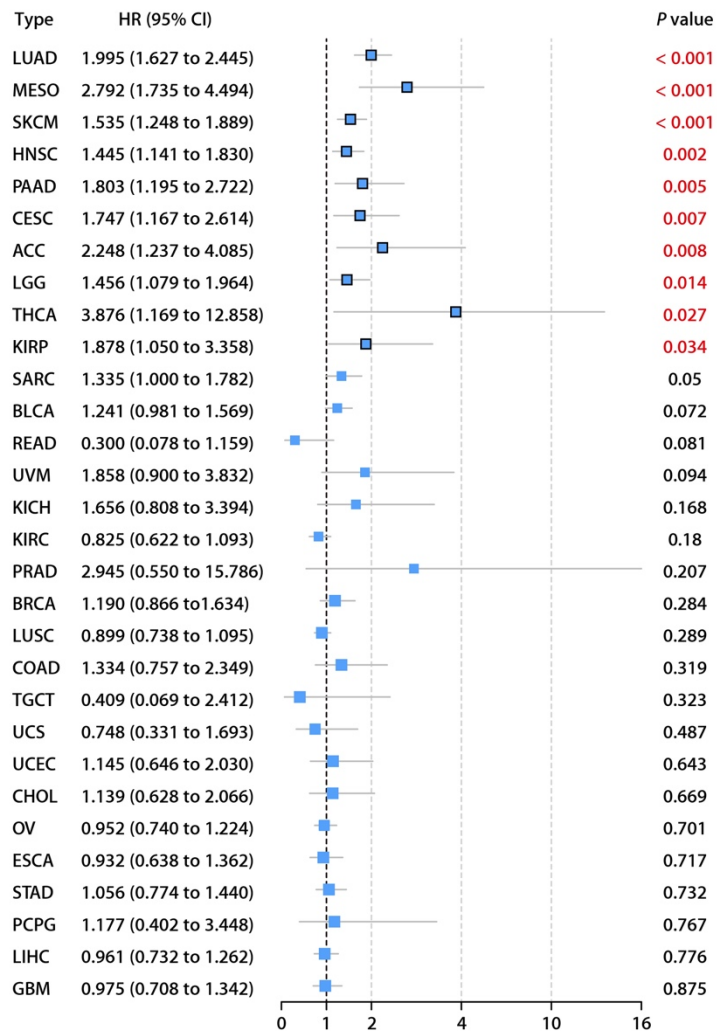
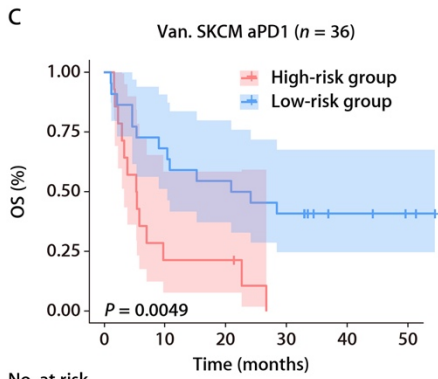
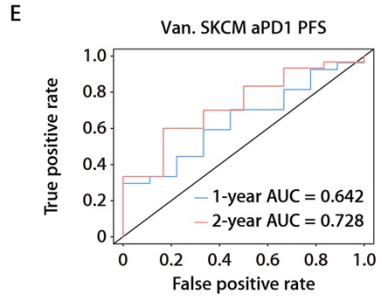
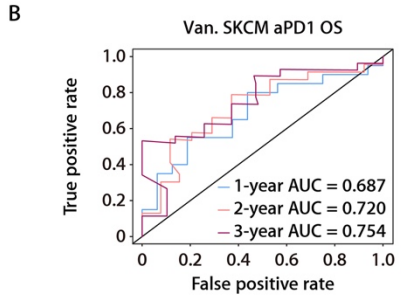
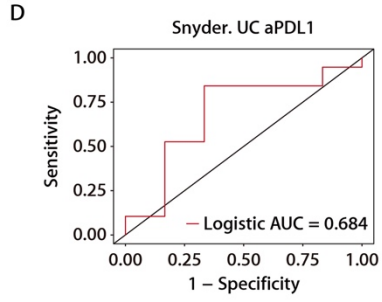
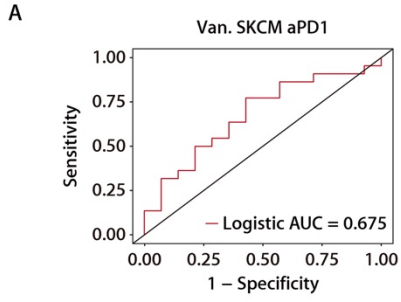


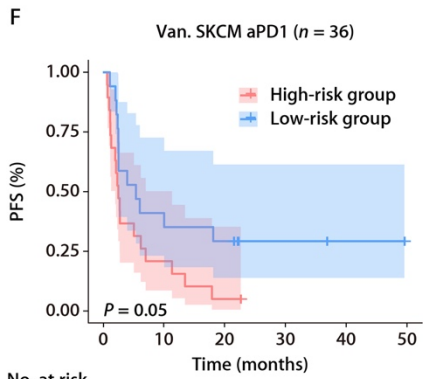
Fig. S4. Multivariate Cox regression analysis of the ROS-related signature in TCGA pan-cancer cohorts.

Forest plot showing hazard ratio (HR) of the ROS-related signature on the OS in TCGA pan-cancer cohort. Error bars are 95% confidence intervals.



No. at risk

High-risk	14	3	3	0	0	0
Low-risk	22	15	12	9	4	2



No. at risk

High-risk	19	4	1	0	0	0
Low-risk	17	7	5	2	1	0

Fig. S5. Prediction of ICI outcome using the ROS-related signature.

(A) ROC plot depicting the performance of the ROS-related signature in the SKCM anti-PD-1 cohort. (B) Time-dependent ROC analysis assessing the predictive function of the ROS-related signature at 1-, 3- and 5-year OS in SKCM anti-PD-1 cohort. (C) K-M survival analysis of OS between the high- and low-risk groups in the SKCM anti-PD-1 cohort. (D) ROC plot depicting the performance of the ROS-related signature in the UC anti-PD-L1 cohort. (E) Time-dependent ROC analysis to assess the predictive function of the ROS-related signature at 1- and 2-year PFS in the SKCM anti-PD-1 cohort. (F) K-M survival analysis of PFS between the high- and low-risk groups in the SKCM anti-PD-1 cohort.

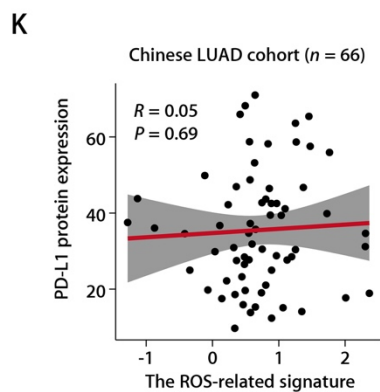
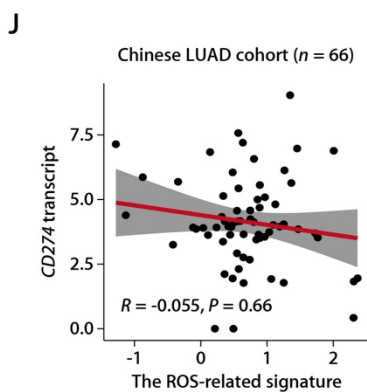
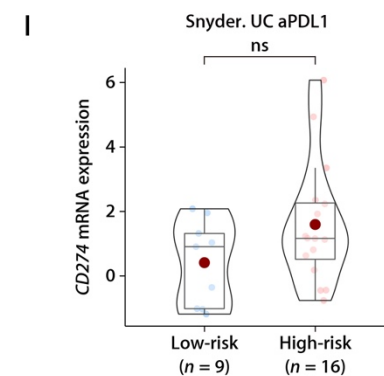
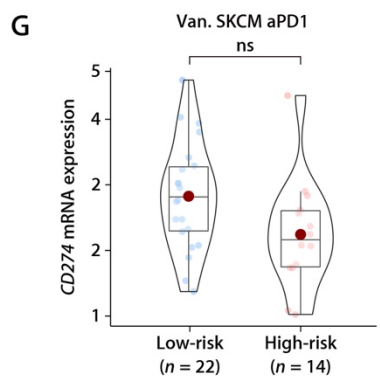
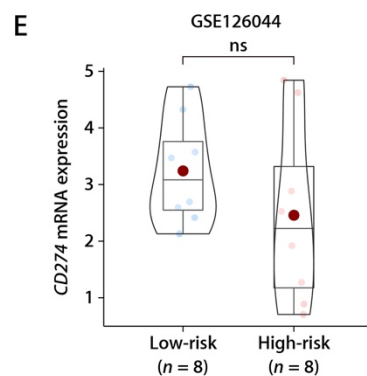
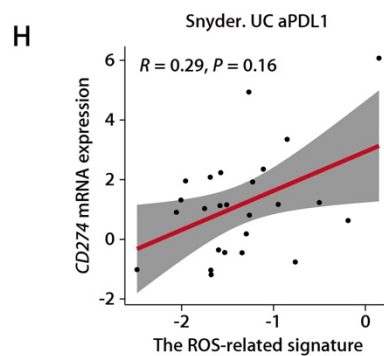
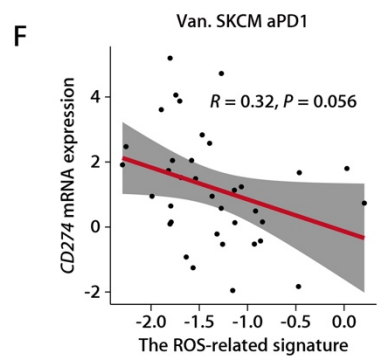
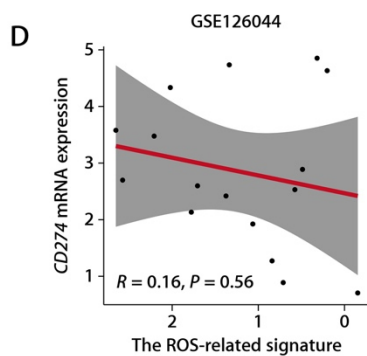
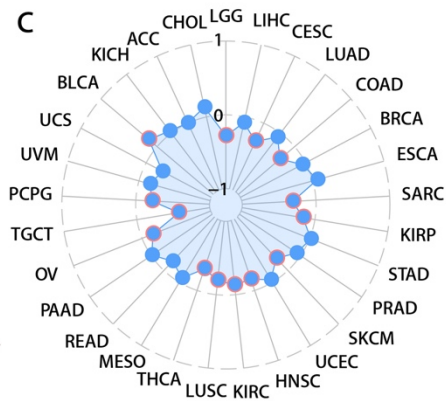
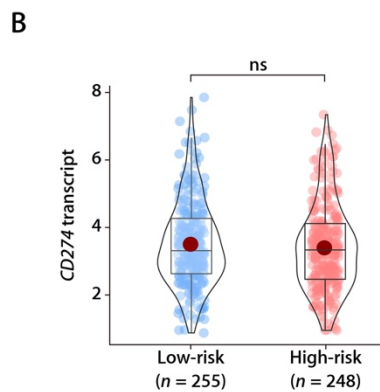
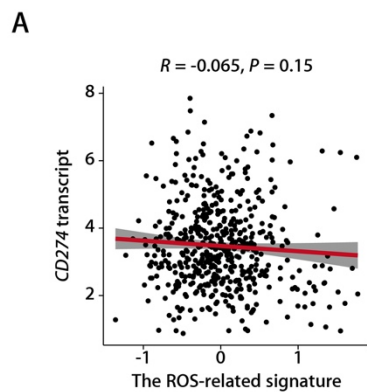


Fig. S6. Correlation analysis of the ROS-related signature and PD-L1 expression.

(A) Correlation analysis between the ROS-related signature and *CD274* mRNA expression in TCGA-LUAD cohort. (B) The distributions of *CD274* mRNA expression between the high- and low-risk groups in TCGA-LUAD cohort. (C) Circos plot depicting the Pearson correlation between the ROS-related signature and *CD274* mRNA expression in TCGA pan-cancer cohorts. The red circle indicates a significant correlation. (D) Correlation analysis between the ROS-related signature and *CD274* mRNA expression in the GSE126044 NSCLC anti-PD-1 cohort. (E) The distributions of *CD274* mRNA expression between the high- and low-risk groups in the GSE126044 NSCLC anti-PD-1 cohort. (F) Correlation analysis between the ROS-related signature and *CD274* mRNA expression in the SKCM anti-PD-1 cohort. (G) The distributions of *CD274* mRNA expression between the high- and low-risk groups in the SKCM anti-PD-1 cohort. (H) Correlation analysis between the ROS-related signature and *CD274* mRNA expression in the UC anti-PD-L1 cohort. (I) The distributions of *CD274* mRNA expression between the high- and low-risk groups in the UC anti-PD-L1 cohort. (J) Correlation analysis between the ROS-related signature and *CD274* mRNA expression in the Chinese LUAD cohort. (K) Correlation analysis between the ROS-related signature and PD-L1 protein expression quantified by IHC analysis in the Chinese LUAD cohort.

Fig. S7. Correlation analysis of the ROS-related signature and immune checkpoint genes.

Heatmap depicting the correlation between the ROS-related signature and the expressions of immune checkpoint genes in TCGA-LUAD cohort.

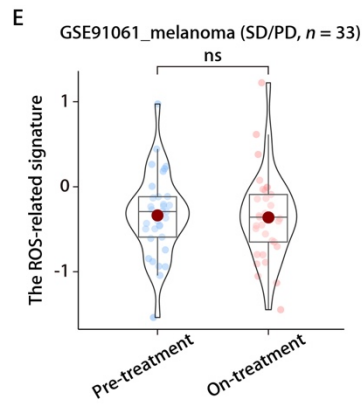
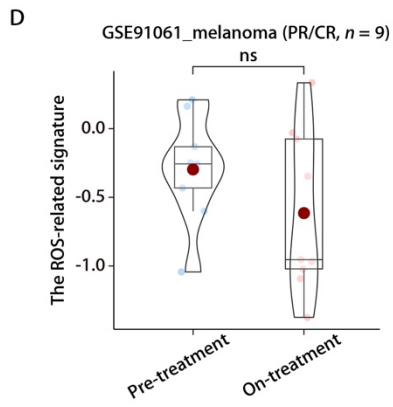
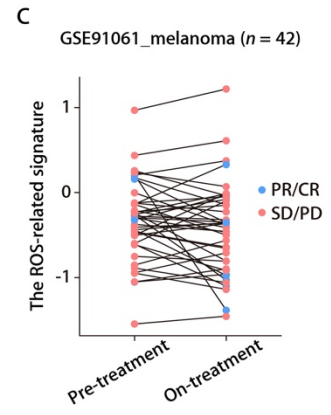
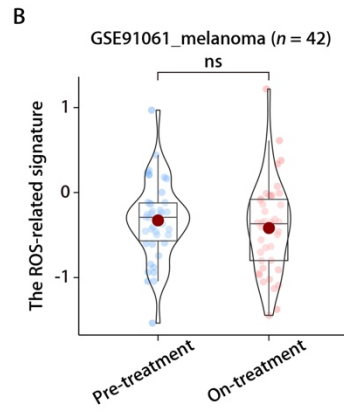
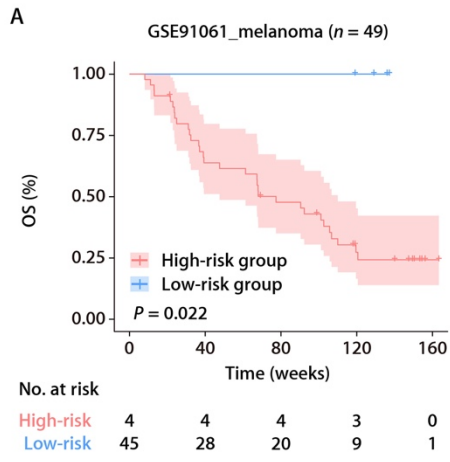


Fig. S8. The association of the ROS-related signature with the primary resistance to immunotherapy.

(A) K-M survival analysis of OS between the high- and low-risk groups stratified by the ROS-related signature in the GSE96061 melanoma immunotherapy cohort. (B) The distributions of the ROS-related signature expression between the pre- and on-treatment samples of patients in the GSE96061 melanoma immunotherapy cohort. (C) Comparison of the ROS-related signature expression between tumor samples of response ($n = 9$) and non-response ($n = 33$) to immunotherapy in the GSE91061 melanoma immunotherapy cohort. (D) The distributions of the ROS-related signature expression between the pre- and on-treatment samples of patients with response to immunotherapy in the GSE96061 melanoma immunotherapy cohort. (E) The distributions of the ROS-related signature expression between the pre- and on-treatment samples of patients with no response to immunotherapy in the GSE96061 melanoma immunotherapy cohort.